

## Modelling, Stack and Imaging: Marine Seismics

Anderson B. Gomes\*, Lourenildo W. B. Leite\*, Leandro Sadala\*, Reynam Pestana\*\*, Gary Aldunate\*\*, Jürgen Mann\*\*\*

(\*) UFPA, (\*\*) UFBA, Brazil, (\*\*\*) Universität Karlsruhe, Germany

Copyright 2007, SBGf - Sociedade Brasileira de Geofísica

This paper was prepared for presentation at the 10<sup>th</sup> International Congress of the Brazilian Geophysical Society, held in Rio de Janeiro, Brazil, November 19-22 2007.

Contents of this paper were reviewed by the Technical Committee of the 10<sup>th</sup> International Congress of The Brazilian Geophysical Society and do not necessarily represent any position of the SBGf, its officers or members. Electronic reproduction or storage of any part of this paper for commercial purposes without the written consent of The Brazilian Geophysical Society is prohibited.

### Abstract

**This paper summarizes practical aspects of seismic modelling of a marine geological ambient of petroleum exploration of passive sedimentary basins along the Brazilian coast. The results of a consistent attention to stack and imaging demonstrate the basics and the potential of the combined SU/WIT processing systems. The central attention is grounded on the data driven CRS (Common Reflection Surface) stack, as we also look at to establish a workflow for seismic reevaluation of sedimentary basins. The CRS stack is attractive because it is a velocity independent method, and is founded on recovered wave front attributes. Using these attributes, a post-stack Kirchhoff type time migration is automatically carried out.**

### Introduction

Obtaining a sufficiently accurate image, either in time or in depth domain, is often a difficult task in regions governed by complex geological structures and/or complicated near surface conditions. Under such circumstances, where simple model assumptions may fail, it is of particular importance to extract as much information as possible directly from the measured data. Fortunately, the ongoing increase in available computing power makes data-driven approaches feasible which, therefore, have increasingly gained in relevance during the last years.

The Common Reflection Surface (CRS) stack (Mann, 2001 and 2002) is one of the method used to improve zero-offset simulation, and to obtain kinematic wavefield attributes as by-products of the data-driven stacking process. As has been shown, they can be both applied to improve the stack itself, and to support subsequent processing steps (Hubral, 1999).

The major steps of this workflow are displayed in Figure 1. The CRS stack based seismic imaging makes use of these extended possibilities by considering 3-D data, smooth and rugged survey topography, by using a parallel processing technology. Heilmann et al. (2004) is a basic reference for the present CRS-stack data-driven imaging strategy.

A fundamental point for good CRS-stack results is the preprocessing of the multicoverage seismic reflection data. The preprocessing was defined as the tasks performed beginning with the geometry setup, muting of top of traces

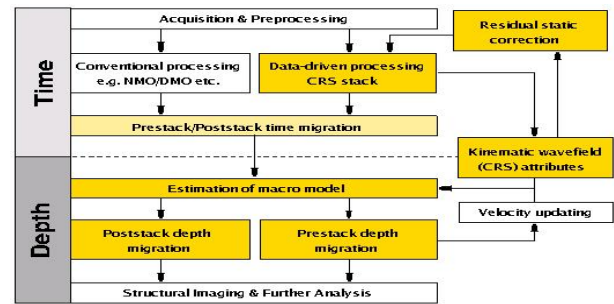


Figure 1: Major steps of the seismic data processing in time and depth domain. Imaging procedures that can be incorporated in the CRS stack based imaging workflow are highlighted in yellow.

and amplitude correction for displaying. These tasks were followed by an imaging sequence consisting of stacks, and of Kirchhoff type time migration based on the CRS attributes. For complementary information to the main steps of the CRS-stack based seismic imaging workflow, other conventional processes were carried out for analysis.

### Method

In conventional coherence velocity analysis, a first problem is related to the representation of the field of seismic waves, and a second problem is related to the criterion for expressing in quantitative form the degree of fitting between the model and the data for a certain stacking velocity. From the algorithm point of view, the velocity analysis procedure in the  $(x, t)$  domain can consist of two steps to be repeated at each point  $t_0$  for every stacking velocity  $v$ : the normal moveout correction, and the coherency summation; both composing the velocity spectrum. Usually, velocity analysis is performed on common-mid-point gathers by approximating the two-way travel time,  $t(x; t_0, v)$ , of primary reflection arrivals of a single interface by a second order hyperbolic function as:

$$t^2(x; t_0, v) = t_0^2 + \frac{x^2}{v^2} + O(x^4). \quad (1)$$

where  $x$  stands for the source-receiver offset,  $t_0$  for the normal two-way travel time for  $x = 0$ , and  $v$  the stack velocity. The above law is ideal for single homogeneous layer and horizontal reflector. For the next complexity of the model, we can compose an ideal medium of multiple homogeneous layers with horizontal interfaces and small apertures, and the above law is still of high approximation (Ursin, 1982). Turning to more real Earth, the underground geology is described by a 3-dimensional variation of velocity that can be smooth or with discontinuities formed

by curved interfaces, what establishes limitations on the use of the above model. For practical conventional use, we need the definition of a well-determined stacking velocity distribution, and the interval velocities can be recovered on the assumption that the stacking velocity  $v$  is approximately equal to the root-mean-square (rms) velocity  $v_{rms}$  (Al-Chalabi, 1974).

The seismic data here used has been produced by finite difference methods from a marine velocity model of the Brazilian marginal basins, where the exploration for oil and gas is of major importance. Many reports bring attention to the presence of vulcanism and saline tectonics in these basins (Chang et al., 1988; Milani et al., 2000).

Results of the 1-D SU/NMO stack is presented in Figure 2. The NMO and a near common-offset section were used for control of the initial simulated CRS stacks. It is expected in these stacks procedures that subsurface structures be represented by visual reflector patterns, as can be seen from many details like ocean bottom line, stratification, anticlines, multiples, free surface faults and local bodies.

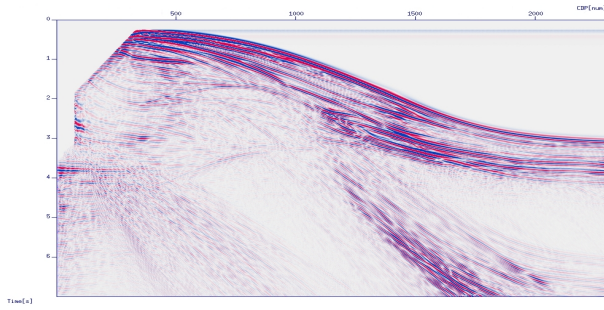


Figure 2: NMO zero offset section simulated by CWP/SU 1-D stack. It is observed many details like ocean bottom line, stratification, anticlines, free surface multiples, faults and local bodies.

The CRS stack procedure takes into account a more complex reflector geometry, but it is not so simple and direct to perform a velocity analysis at a first glance. Following Schleicher and Hubral (1993), based on the paraxial ray theory, the 2-D hyperbolic operator, as an approximation for the two-way traveltime of primary reflections from a curved interface with reference to a flat observation surface is given by:

$$t_{hyp}^2(x_m, h) = \left[ t_0 + \frac{2 \sin \alpha_0 (x_m - x_0)}{v_0} \right]^2 + \frac{2 t_0 \cos^2 \alpha_0}{v_0} \left[ \frac{(x_m - x_0)^2}{R_N} + \frac{h^2}{R_{NIP}} \right]. \quad (2)$$

where it is assumed that the velocity  $v_0$  is known and related to an upper layer around the observation point  $x_0$ . The independent variables  $x_m$  and  $h$  are, respectively, the midpoint and half offset in the CMP configuration, and  $x_0$  is the reference point of stack. The parameter  $\alpha_0$  corresponds to the vertical emergence angle of the wavefront at the observation point. The quantities  $R_{NIP}$  and  $R_N$  are related to the central ray in the paraxial ray theory. The CRS stack has the form of a macro-model independent stacking method to simulate a zero-offset section in the  $(x, t)$  domain. The operator is obtained considering two theoretical experiments are performed to generate eigenwaves: the NIP-wave and the N-wave. The first wave is associated with an exploding diffractor to

produce the normal incidence point wave of radius  $R_{NIP}$  at the surface of observation. The second wave is associated with the exploding reflector to generate the normal wave of radius  $R_N$  at the surface of observation, being the exploding reflector locally approximated by a segment of an arc of circle around the NIP point. In order to satisfy the paraxial ray theory, a central ray of information has to be established, and in this case it is taken the zero offset ray between the observation point and the normal incidence point (normal ray), and only primary events are taken into account. The central ray satisfies Snell's law across the interfaces, and the wavefront curvatures of the NIP-wave and N-wave change according to the refraction and transmission laws of curvature.

For the goodness of fit, numerous functionals have been proposed to be evaluated quantitatively on a given CMP gather for a certain stacking velocity (Sguazzero and Vesnaver, 1987). The most common functionals measure the likeness of the NMO corrected gather's amplitude traces ( $\bar{u}$ ) based on summation or correlation of traces, and choices of normalization. The normalized measure Semblance  $S(v; t_0)$  provides NMO corrected traces, from a near first  $x = x_F$  to a last  $x = x_L$  offset with  $N_x$  points, and in a time window specified by some  $\delta$ .  $S(v; t_0)$  takes values in the interval (0,1) regardless of the signal amplitude, and it quantifies the uniformity of the signal polarity across the NMO corrected gather amplitude  $\bar{u}(v; t_0)$ . In the NMO stack, the function  $S(v; t_0)$  can also be interpreted as the function to be optimized, from where the optimum value of the stack velocity results.

The CRS stack uses the CWP/SU environment, and it takes the integer data header format to use the source,  $x_S$ , and receiver,  $x_G$ , coordinates, and the scale, along with the information for the  $x_m$  and  $h$  coordinates given by:  $x_m = \frac{(x_S + x_G)}{2}$  and  $h = \frac{(x_S - x_G)}{2}$ . The reference point of stack is represented by  $P_0(x_0, t_0)$ , and the stack trajectories are over the coordinates  $h$  and  $x_m$ .

Results of the CRS stack start with the coherence function depicted in Figure 3. This function controls the estimation of the CRS stack attributes for the point stacks  $P_0(x_0, t_0)$ . It is expected that subsurface structures to be represented by tendency patterns, and the better images are given by stronger of patterns continuity and higher values of coherence.

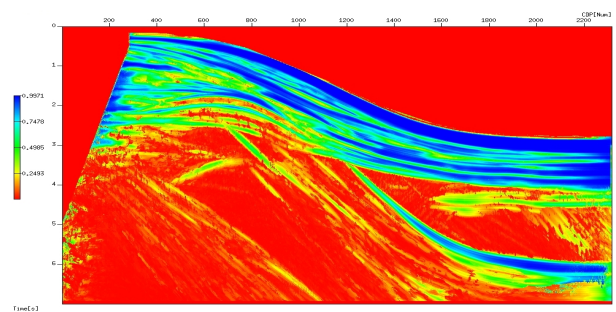


Figure 3: Coherence function for the marine line. Observe the pattern trends and the free surface multiples.

The time panels of kinematic CRS wavefield attributes, version 2D for flat observation surface, as shown in Figures 4, 5, and 6 are, respectively, the following: (1) a section

of the emergence angle  $\alpha_0$  of the zero-offset normal ray with respect to the normal to the measurement surface; (2) a section of the radius of curvature  $R_{NIP}$  of the wavefront relative to point source experiment at the normal incidence point (NIP) as observed at the emergence point of the normal ray; and (3) a section of the curvature  $R_N$  of the normal wavefront due to an exploding reflector element at the NIP. Coherence sections are used to identify locations with very low values since such locations are not expected to be associated with reliable attributes. The sections of  $\alpha_0$  and  $R_{NIP}$  are used to obtain stacking velocity sections.

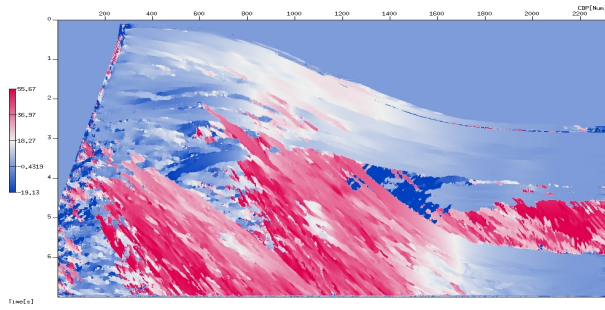


Figure 4: CRS attribute: Angle panel,  $\alpha_0$ . Observe a rather simple distribution of values with very strong structural patterns.

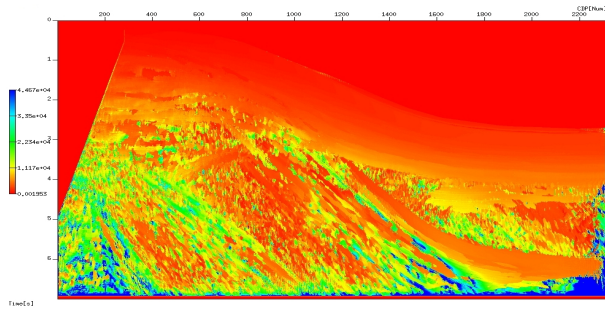


Figure 5: CRS attribute: Rnip panel. As in the previous panel, observe a rather simple distribution of values with very strong patterns.

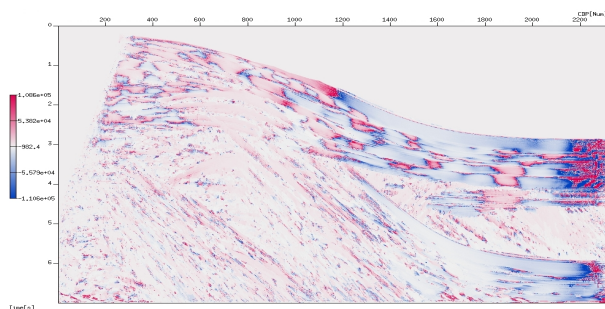


Figure 6: CRS attribute: Rn panel. Not as clear as the previous ones, observe a rather simple distribution of values with strong patterns.

Figure 7 displays the basic simulated CRS ZO panel. Near common-offset gathers were also used to help analyse the

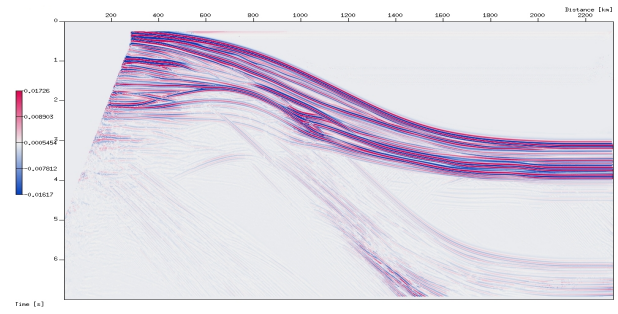


Figure 7: Optimized zero offset section simulated by CRS stack. A Fresnel window result can be also simulated. Besides the high resolution, it is observed many details like ocean bottom line, stratification, anticlines, free surface multiples, faults and local bodies.

difficulties in interpreting underlying reflections in the ZO sections.

The approximated diffraction response might be used as alternative stacking operator to simulate a ZO section with Kirchhoff-type operators, although the CRS operator better approximates the actual reflection events. An attractive application was proposed by Mann (2002), where the apex of the appropriate diffraction response also provides an approximation of the image location of a Kirchhoff time migration. Due to the symmetry axis, this applies to the ZO plane  $h = 0$ , where  $\partial t_D(x_m, h = 0) / \partial x_m = 0$  yields the apex location:

$$x_{apex} = x_0 - \frac{R_{NIP} t_0 v_0 \sin \alpha}{2R_{NIP} \sin^2 \alpha + t_0 v_0 \cos^2 \alpha}, \quad (3)$$

$$t_{apex}^2 = \frac{t_0^3 v_0 \cos^2 \alpha}{2R_{NIP} \sin^2 \alpha + t_0 v_0 \cos^2 \alpha}. \quad (4)$$

Parameterized in terms of the apex location  $(x_{apex}, t_{apex})$ , instead of the ZO location  $(x_0, t_0)$ , and with  $h = 0$ , the approximate ZO diffraction response reads:

$$t_D^2(x) = t_{apex}^2 + \frac{4(x - x_{apex})^2}{v_c^2} \quad \text{with} \quad (5)$$

$$v_c^2 = \frac{2v_0^2 R_{NIP}}{2R_{NIP} \sin^2 \alpha + t_0 v_0 \cos^2 \alpha}. \quad (6)$$

A summation along the approximate diffraction response with its result assigned to its apex approximates a Kirchhoff time migration with a constant velocity  $v_c$ , where all the attributes contribute. In the strategy used, the stack is performed along the CRS operator instead of the diffraction operator, and assign the result to the apex  $(x_{apex}, t_{apex})$ . Figure 8 shows the result of the CRS Kirchhoff-type time migration, which is automatic and fast. It is obtained from the optimized zero offset section simulated by CRS stack. It is observed a scatter of points due to noise in the attributes. But, it is still observed many details like the ocean bottom line, stratification, anticlines, multiples, faults and local bodies.

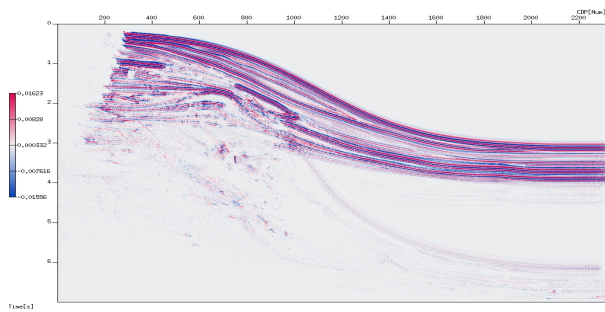


Figure 8: CRS Kirchhoff type time migration. This result is rather automatic and fast computed, and it is obtained from the optimized zero offset section simulated by CRS stack. It is observed a scatter of points due to noise in the attributes. But, it is still observed many details like the ocean bottom line, stratification, anticlines, free surface multiples, faults and local bodies.

### Summary and Conclusions

A rather long synthetic time section was intentionally processed without cuts. The intention was to check also on some geometrical resolution of geological structures present in the model. Considering the limitations of the coloured figures, interpretation should be carried out mainly on the basis of the stack and migration time sections. It is important that the maps have the proper scale, axis exaggeration and size. From screen display and details of these figures, discontinuities, a major anticline, faults and free surface multiple can be identified. The left and right parts of the section do not show problems with external multiples that are the major concern in the central part of the section, and related to the continental slope.

The quality of the marine synthetic seismic data does not impose a strong limitation in enhancing different parts for imaging a seismic line. The intention is to present in the course of the studies the processing of field lines to provide better grounds for geological interpretation of real data. Also, to demonstrate the applicability of the CRS-stack based imaging as a system towards basin reevaluation providing good basis for geological interpretation, and hopefully for a successful drilling.

The coherence sections serve to indicate the data-driven estimated fit between the CRS stacking operators and primary reflection events in the CMP gather. It is noticeable that the overall seismic image quality is good, but taking into account data quality that served as reference for the projects being carried out in the institution. The results obtained by CRS stack revealed good resolution as measured by signal-to-noise ratio and reflector continuity.

The reliability and quality of the results of the CRS-system based seismic imaging workflow is once more demonstrated, and it can be further advanced and broadened with respect to the studies in focus.

This example serves to reinforce our perspectives and intentions on research collaboration between different Universities, and between University and Industry to provide development and human resources for the established seismic exploration technology.

### References

- Al-Chalabi, 1974, An analysis of stacking (RMS) average and interval velocities over a horizontally layered ground, *Geophysical Prospecting*, Vol. 22, No. 03, p. 458-475.
- Chang, H. K., Kowsmann, R. O., Figueiredo, A. M. F., 1988, New development of East Brazilian Marginal Basins. Episodes. *International Geoscience Newsmagazine*, Vol. 11, No. 3, p. 194-202.
- Heilmann, Z., Mann, J., Duvencek, E. and Hertweck, T., 2004, CRS-stack-based seismic reflection imaging: a real data example, *Extended Abstracts, 66th EAGE Conference and Exhibition*, Paris, France.
- Hubral, P., 1999, Macro-model Independent Seismic Reflection Imaging (special issue), *Journal of Applied Geophysics*, Vol. 42, No. 3-4.
- Mann, J., 2001, *Common-Reflection-Surface Stack: User's manual to version 4.2*, Geophysical Institute, University of Karlsruhe.
- Mann, J., 2002, *Extensions and Applications of the Common-Reflection-Surface Stack Method*, Institute of Geophysics, University of Karlsruhe, Germany.
- Milani, E. J., Brandão, J. A. S. L., Zalán, P. V. and Gamboa, L. A. P., 2000, *Petróleo na margem continental brasileira: geologia, exploração, resultado e perspectivas*. *Revista Brasileira de Geofísica*, Vol. 18, No. 3, p. 1-21.
- Schleicher, J., Tygel, M., and Hubral, P., 1993, Parabolic and hyperbolic paraxial two-point traveltimes in 3D media, *Geophysical Prospecting*, Vol. 41, No. 4, p. 495-514.
- Sguazzero, P. & Vesnaver, A., 1987, A comparative analysis of algorithms for stacking velocity estimation. In: Bernabini et al. *Deconvolution and Inversion*. Blackwell Scientific Publications. London.
- Ursin B., 1982, Quadratic wavefront and traveltimes approximations in inhomogeneous layered media with curved interfaces, *Geophysics*, Vol. 47, No. 7, p. 1012-1021.

### Acknowledgments

We would like to thank ANP, PETROBRAS, FINEP and CNPq for the research support and scholarships, and WIT Consortium for the continuous attention and support.